LIMNOLOGY and OCEANOGRAPHY

ASLO

Limnol. Oceanogr. 68, 2023, 2749–2758

doi: 10.1002/lno.12461

Size and transparency influence diel vertical migration patterns in copepods

Alex Barth [1*] **Rod Johnson,** [2] **Joshua Stone** [1]

[1]University of South Carolina, Biological Sciences, Columbia, South Carolina, USA
[2]Bermuda Institute of Ocean Sciences, Bermuda, UK

Abstract

Diel vertical migration (DVM) is a widespread phenomenon in aquatic environments. The primary hypothesis explaining DVM is the predation-avoidance hypothesis, which suggests that zooplankton migrate to deeper waters to avoid detection during daylight. Copepods are the predominant mesozooplankton undergoing these migrations; however, they display massive morphological variation. Visual risk also depends on a copepod's morphology. In this study, we investigate hypotheses related to morphology and DVM: (H1) as size increases visual risk, increases in body size will increase DVM magnitude and (H2) if copepod transparency can reduce visual risk, increases in transparency will reduce DVM magnitude. In situ copepod images were collected across several cruises in the Sargasso Sea using an Underwater Vision Profiler 5. Copepod morphology was characterized from these images and a dimension reduction approach. Although in situ imaging offers challenges for quantifying mesozooplankton behavior, we introduce a robust method for quantifying DVM. The results show a clear relationship in which larger copepods have a larger DVM signal. Darker copepods also have a larger DVM signal, however, only among the largest group of copepods and not smaller ones. These findings highlight the complexity of copepod morphology and DVM behavior.

Diel vertical migration (DVM) is a wide spread phenomenon with large consequences in ocean ecosystems. DVM is the process of pelagic organisms vertically moving in the water column on a daily basis, often traveling dozens to hundreds of meters (Bianchi and Mislan. 2016). This large-scale event occurs across many taxa, from plankton to fish (Brierley 2014). However, DVM is particularly notable in zooplankton communities, whose migrations contribute substantially to biogeochemical cycles (Steinberg and Landry 2017; Archibald et al. 2019; Siegel et al. 2023). Mesozooplankton communities, largely dominated by copepods (Turner 2004), will feed in surface layers of the ocean at night then migrate into deeper waters during daytime. Through this movement, copepods actively transport carbon to depth. In addition, Kelly et al. (2019) described zooplankton DVM to be a major component of mesopelagic food webs. Thus, to understand pelagic food webs and nutrient cycles, it is critically important to understand the drivers of DVM.

DVM has long been studied in marine systems (Bandara et al. 2021). Predominantly, zooplankton DVM is the movement from deep waters at daytime to shallower waters at night (Hays 2003; Bianchi and Mislan. 2016). However, reverse migration is also well documented (Ohman 1990). The adaptive benefits of DVM have been extensively reviewed (Lampert 1989; Hays 2003; Cohen and Forward Jr. 2009; Ringelberg 2009; Williamson et al. 2011; Bandara et al. 2021). Some studies have hypothesized that DVM provides a physiological advantage. It has been suggested that moving to deeper waters may provide zooplankton a reduction in UV damage (Ewald 1912; Kessler et al. 2008), metabolic benefits (McLaren 1963; Enright 1977), or demographic benefits (McLaren 1974). However, the predator-avoidance hypothesis has received the most support to explain ultimate causes of DVM (*see* review of current evidence by Bandara et al. 2021). First described by Zaret and Suffern (1976), this hypothesis posits zooplankton evacuate the sunlit surface to evade visual predators then ascend at night to feed. However, the massive migration undertaken by zooplankton is energetically expensive (Maas et al. 2018; Robison et al. 2020). Therefore, the predator-avoidance hypothesis makes a clear prediction that the trade-off of expended energy is worth the

*Correspondence: ab93@email.sc.edu

Additional Supporting Information may be found in the online version of this article.

Author Contribution Statement: AB and JS developed the study hypotheses. JS coordinated deployment and data management of the UVP. RJ facilitated data collection on cruises. AB led the analysis and preparation of the manuscript and figures. JS and RJ contributed to the manuscript draft. All authors approved the final submission.

predator avoidance benefit (Lampert 1989). This trade-off has been further described in observations of the relationship between zooplankton feeding and DVM patterns which led to the hunger-satiation hypothesis (Atkinson et al. 1992; Pearre 2003). This hypothesis suggests that vertical migrators will ascend to feed when hungry then retreat once full. Once an individual has fully fed, remaining at the surface provides no benefit while their visual risk may increase due to their full guts which may increase visibility. Thus, the hunger-satiation hypothesis provides a detailed case of the predator-avoidance hypothesis and suggests cases where copepods may forego DVM. Regardless, both the hunger-satiation hypothesis and the predator-avoidance hypothesis suggest DVM is primarily a result of top-down control. In modeling studies with copepods, the predominant oceanic zooplankton, top-down control (Bandara et al. 2019) and trophic interactions (Pinti et al. 2019) have successfully been used to replicate DVM patterns.

Predator-driven migration suggests that DVM can be a function of an individual copepod's detection risk by a visual predator. However, this risk can depend on a copepod's morphological features (Aksnes and Utne 1997). Notably a copepod's size can increase visual detection. Several studies have documented that copepod size influences DVM magnitude (Hays et al. 1994; Ohman and Romagnan 2016; Aarflot et al. 2019). Presumably, a copepod's transparency will also influence DVM. Hays et al. (1994) reported that pigmentation explained variation in DVM frequency. However, few other studies have investigated this at length. One barrier to studying a relationship between copepod morphology and DVM is the difficulty of accurately recording traits. Several approaches have been utilized to study DVM. High spatiotemporal resolution of DVM can be achieved through acoustic (Liu et al. 2022), and even satellite-based measurements (Behrenfeld et al. 2019). However, these approaches do not yield information about individuals, much less traits. Net collected specimens can allow for trait-related investigations of copepod DVM patterns (Hays et al. 1994; Ohman and Romagnan 2016). However, it is much more challenging to measure traits related to copepod transparency from net-collected specimens. Copepods collected from deep net tows can be severely damaged and their gut contents may not reflect natural conditions due to cod-end feeding or regurgitation. Furthermore, typical preservation methods of net-specimens can result in the loss of pigmentation through bleaching in ethanol or formalin or increases in opacity as the copepod dies. Yet traits related to copepod's transparency are not well captured in net-collected specimens which may evacuate gut contents or lose pigmentation following preservation in formalin or ethanol. In Hays et al.'s (1994) investigation, the authors relied on previously published copepod carotenoid values in their analyses rather than attempt to measure pigment values from their preserved specimens.

However, these sampling challenges may be effectively circumvented with the emerging use of in situ imaging tools. By directly observing copepods, new insights into their behavior and traits can be resolved (Ohman 2019). For example, Whitmore and Ohman (2021) used an in situ imaging device to describe a relationship between copepod abundance with a particulate field rather than chlorophyll *a*. Such findings are facilitated by the fact imagery data records an individual's exact position. In addition, a copepod's true appearance, including difficult to record metrics like transparency, can be measured. Thus, in situ imaging offers a new perspective to investigate DVM hypotheses. Some studies observed a copepod DVM pattern with in situ imagery data (Pan et al. 2018; Whitmore and Ohman 2021). However, direct tests of DVM-related hypotheses with such data have not yet been conducted.

In this study, we utilized in situ imaging to evaluate how copepod morphological traits influence DVM patterns. We specifically test the hypotheses that (H1) as size increases visual risk, increases in body size will increase DVM magnitude and (H2) if copepod transparency can reduce visual risk, increases in transparency will reduce DVM magnitude. If these morphologically based hypotheses are true, then the larger and darker copepods will have the largest DVM magnitude.

Methods

CTD profiles and Underwater Vision Profiler imaging of copepods

Data were collected aboard the R/V Atlantic Explorer in collaboration with the Bermuda Atlantic Time-series Study (BATS) (Steinberg et al. 2001). In situ images of plankton were acquired using an Underwater Vision Profiler 5 (UVP5) (Picheral et al. 2010). The original sampling methodology and instrument specification followed details described in Barth and Stone (2022). The UVP was attached to the Conductivity-Temperature-Depth profiling rosette (CTD) and deployed regularly on cruises to the Sargasso Sea from June 2019 to December 2021. Typical monthly cruises included 13 profiles with average descents to 1200 m (Supplementary Fig. S1). In this study, we investigated general trends in DVM by pooling together casts across multiple cruises. This approach is necessitated by the small sampling volume of the UVP (1.1 liters per image) and low abundance of plankton which requires aggregation of data to resolve trends (*see* details in Barth and Stone 2022). Although there was minor variation between cruises (Supplementary Fig. S2), this oligotrophic system is relatively consistent across seasons (Steinberg et al. 2001). In addition, every cruise had an approximately equal number of day and night casts. Profiles were assigned to be day or night based on locally calculated nautical dawn and nautical dusk times using the R package `suncalc 0.5.1`.

The UVP records images of large particles (> 600 μm equivalent spherical diameter [ESD]). However, living particles are not reliably identifiable below 900 μm (Barth and Stone 2022). All recorded images were processed using Zooprocess (Gorsky et al. 2010), which provides several metrics related to size, gray value, and shape complexity. These features were then used to

automatically sort images using Ecotaxa (Picheral et al. 2017). All images were manually verified by the same trained taxonomist. In total, 294,913 images were recorded. Of these, 85.2% were images of debris or artifacts. The smallest identified copepod was 0.940 mm ESD and the largest was 5.904 mm ESD. Across all casts, copepods were the most common organism, composing 58.7% of all identified, living particles. In total, there were 4151 individual copepods images.

Morphological grouping

Zooprocess measures and collects several morphologically relevant parameters. To create relevant groups of copepods, a dimension reduction approach was used. Similar methods have been successfully utilized to provide novel insights to marine snow (Szeligowska et al. 2021; Trudnowska et al. 2021), copepod dynamics in the Arctic (Vilgrain et al. 2021), and temporal trends in phytoplankton communities (Sonnet et al. 2022). First, 18 morphologically relevant parameters were selected to be included in a principal components analysis (PCA), following Vilgrain et al. (2021). Parameters can be described as relating to size (e.g., major axis, ESD), gray intensity (e.g., mean gray value at 625 nm wavelength light), shape (e.g., elongation, symmetry), and shape complexity (e.g., fractal dimension). Gray-value intensity specifically can capture a variety of characteristics related to particle transparency (Gorsky et al. 2010). Note that the UVP5 utilizes a narrow band pass filter set to 625 nm, removing the effect of ambient lighting on particle transparency metrics (Picheral et al. 2010). Feeding these multiple metrics into a morphospace analysis has several advantages. First, principle components establish the major axes of variability which can aid in interpreting the relative importance of different traits. Furthermore, in the context of this study, there are several factors which influence copepod transparency which are not easily distinguishable in most UVP images. If only one metric was selected it may only capture one aspect of transparency, thus by including all factors, we can create a composite metric. Such approaches have been utilized successfully to infer characteristics in in situ imaged marine snow (Szeligowska et al. 2021; Trudnowska et al. 2021).

The PCA was weighted by the volume sampled in a 1-m depth bin for each observation. This approach provides a correction for the UVP's variable descent speed which can cause duplicate imaging of individuals. Although this phenomenon has a minor impact on overall results (Barth and Stone 2022), we used the weighted approach to assure that no individual features were overrepresented. All morphological descriptors were scaled and centered prior to inclusion in the analysis. The model was constructed using the R package `FactoMineR` 2.7. Principal components (PCs) were deemed to be significant if their eigenvalues were greater than 1. This approach yielded four PCs which described 87.3% of the total variation in morphological parameters, with 34.5% and 26.5% in the first two components, respectively. The third and fourth PCs were related to the orientation of the copepod and appendage visibility, respectively. Presumably, this is an artifact of how the copepod was imaged. Because all axes in a PCA are orthogonal to one another, the variation captured by PC1 and PC2 are largely spread evenly across the copepod image variability (PC3 and PC4). This is a particularly useful feature as copepod orientation presumably impacts some metrics such as size and gray-value. Yet, because orientation is largely accounted for with PC3, by grouping along the first two PCs, variation attributable to orientation is homogeneous across those axes.

To address our morphology-DVM hypotheses, we constructed discrete morphological groups based on the first two PCs. Groups along each of the PCs were defined as low (below 25th percentile), mid (25th–75th percentiles) and high (greater than 75th percentile). To address the size-dependent hypothesis (H1), groups were assigned as low, mid, or high along PC1. Then to assess if color/transparency was a secondary factor (H2), within each PC1 group, PC2 groups were constructed as low, mid, or high. In total, this created nine groups (e.g., Low PC1-Low PC2, Low P1-mid PC2, etc.).

Copepod vertical structure and DVM

Vertical distribution of copepods

Copepods in this system are well documented to undergo DVM (Steinberg et al. 2000; Schnetzer and Steinberg 2002; Maas et al. 2018). However, there have not been direct measurements of DVM with in situ imaging data. First, to assess which portion of the water column copepods were utilizing for DVM, we visualized the average vertical structure. The concentrations of each morphological group (based on PC1 and PC2) were calculated in 20-m depth bins for each UVP profile. Profiles were designated as either day or night. Then across all day/night profiles, the mean concentration was calculated for each 20-m depth bin.

Weighted mean depth variability

Weighted mean depth (WMD) is a common metric to describe vertical structure and DVM in zooplankton (Ohman et al. 2002; Ohman and Romagnan 2016; Aarflot et al. 2019). However, with in situ imagery and our particular dataset, this approach presents a few challenges. WMD cannot be calculated individually for each profile then averaged because many profiles in this study had different descent depths. In addition, the small and uneven sampling volume of the UVP can make single casts too variable to reliably resolve abundance. Yet, understanding variation around the WMD is necessary to compare DVM strength across groups. Here, we introduce a depth bin constrained bootstrap approach to define WMD with a 95% confidence interval (CI). To do this, the concentration of each group, was calculated in 20-m depth bins for each profile. Then all profiles were "pooled," separately for day/night. This provides a distribution of concentrations in each depth bin. Pooling across multiple seasons was necessary to have sufficient data; however, it does introduce additionally variability. Due to the different descent speeds and depth of profiles, there are

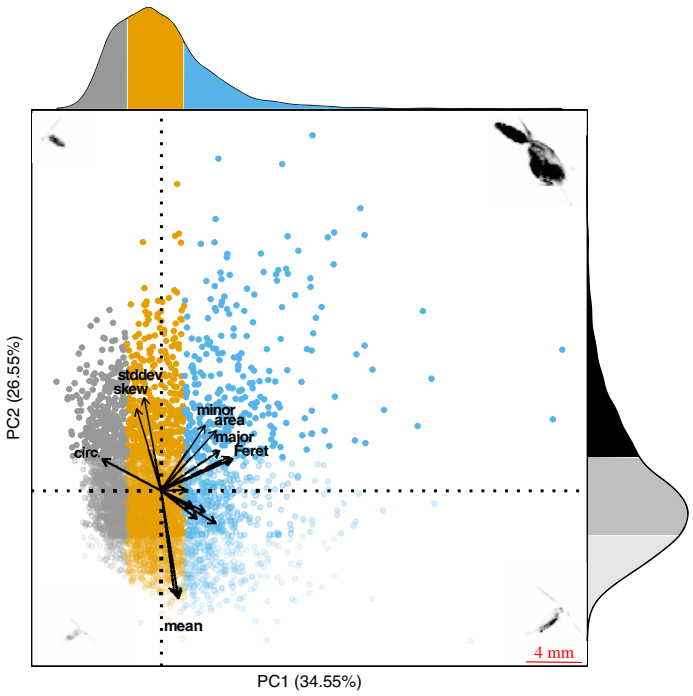

Fig. 1. First two PCs of the morphospace. Proportion of variance explained by the two axis is 61.1%. Each point represents an individual copepod. The color and transparency of each point correspond to the morphological groups based on percentile along each axis. Along PC1, gray corresponds to the low-group (< 25th percentile), orange to the mid group (25th–75th percentiles), and blue to the high-group (75th percentile). Along PC2, low, mid, and high groups are distinguished by increasing opacity. Marginal distribution displays the proportion of observations in each group. Representative vignettes of copepods are shown in the corners corresponding to their place in the morphospace. A 4-mm scale bar in the bottom right is shown for the vignettes.

more observations of surface depth bins. Thus, traditional bootstrapping would bias estimate toward the surface as resampling would be more likely to draw a more-frequently observed surface bin. To avoid this, bootstrap samples were "bin-constrained" such that for each iteration, a random observation was drawn within each depth bin, then replaced for the next iteration. A maximum depth was set to 600 m based on qualitative observations of vertical profiles. This approach effectively created a random profile by resampling a concentration, conc*, from each depth bin, d. For each iteration, the random constructed profile then was used to calculate a bootstrapped weighted mean depth, WMD*. This was done for each morphological group, g, at each time of day, t (day/night).

$$\mathrm{WMD}^*_{g,t} = \sum_{i}^{N=30} \frac{d_i\left(\mathrm{conc}^*_{i,g,t}\right)}{\sum_i^{N=30} \mathrm{conc}^*_{i,g,t}}$$

The distribution of $\mathrm{WMD}^*_{g,t}$ then was used to calculate a bootstrapped mean and 95% CI. The width of the confidence interval then is influenced both by the spread of copepods through the water column and the amount of data available to confidently support their estimates. Thus, this resampling approach is conservative in identifying a significant trend. The conservative approach is desirable given both its robustness to UVP sampling variability and the need to pool casts as described above. To assess a DVM pattern, the 95% CIs can be compared between times of day and morphological groups. We define a clear DVM signal (e.g., significant day/night difference) as when there is no overlap between between the 95% WMD CIs between nighttime and daytime groups. If a clear signal was observed, the DVM magnitude can be measured by comparing the mean WMD*s.

With PC1 to assess the size-based hypothesis (H1), the WMD was compared between the three PC1-groups by percentile level. Then to assess the effect of transparency (H2) the WMD was compared between PC2 groups within each PC1 grouping.

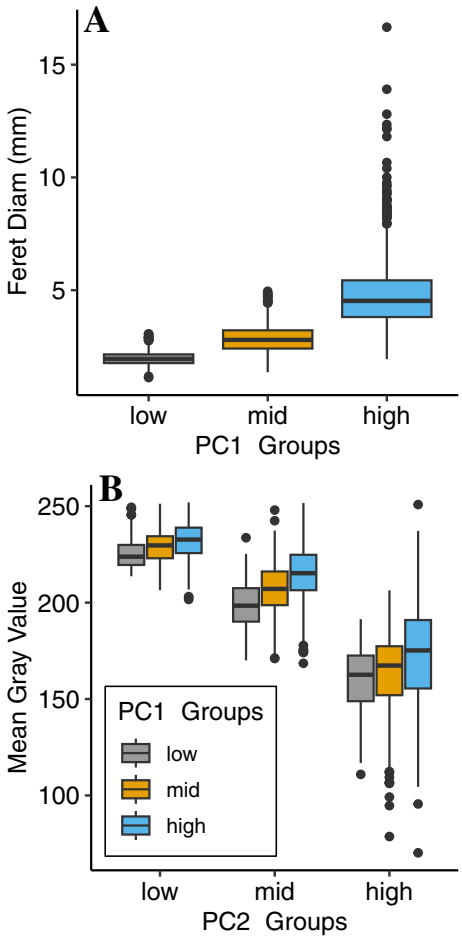

Fig. 2. Comparison of morphological groups to relevant parameters. Groups were constructed along PCs with low as below 25th percentile, mid as 25th–50th percentiles, and high as above 75th percentile. (**A**) PC1 groups are significantly different along Feret diameter and display a clear trend for size. (**B**) PC2 groups are significantly different in terms of mean gray value. Note that a low mean gray value indicates a darker copepod.

Results

Morphological groups

The PCA revealed four major axes of variability (Fig. 1). The first axis (PC1, 34.23% of variability) was largely explained by increasing values related to size, such as perimeter (loading score = 0.927) and Feret diameter (maximum distance between parallel planes around an object) (loading score = 0.910). The second axis (PC2, 27.24% of variability) can be interpreted as a gradient of transparent to dark individuals. PC2 was largely anticorrelated with mean gray value (higher values indicate a more transparent individual) (loading score = −0.920). As noted in the methods, PC3 and PC4 were both related to the orientation of the copepod and the appendage visibility, respectively (Supplementary Fig. S2).

The morphological groupings were assigned along PC1 as low, mid, and high. Then along PC2, groups were assigned within each PC1 group (Fig. 1). To confirm the morphospace grouping resulted in ecologically relevant categories, the morphological groups were compared against known copepod metrics. Across all PC1 groups, there was a clear difference in Feret diameter. The median Feret diameter of the low group was 1.97 mm. The median Feret diameter of the mid and high groups were 2.84 and 4.83 mm, respectively (Fig. 2A). All groups were significantly different from one another (Dunn Kruskall–Wallace test, $p < 0.001$). PC2 groups as a whole were also significantly different from one another (Dunn Krustall–Wallace test, $p < 0.001$). However, within each PC2 group, there was a clear tendency for larger copepods (high PC1 group) to be more transparent (Fig. 2B).

Vertical profiles of morphological groups

For all groups, the 20-m-binned profiles show a notable structure. Although copepods were observed throughout the mesopelagic (Supplementary Fig. S2), the majority of day/night

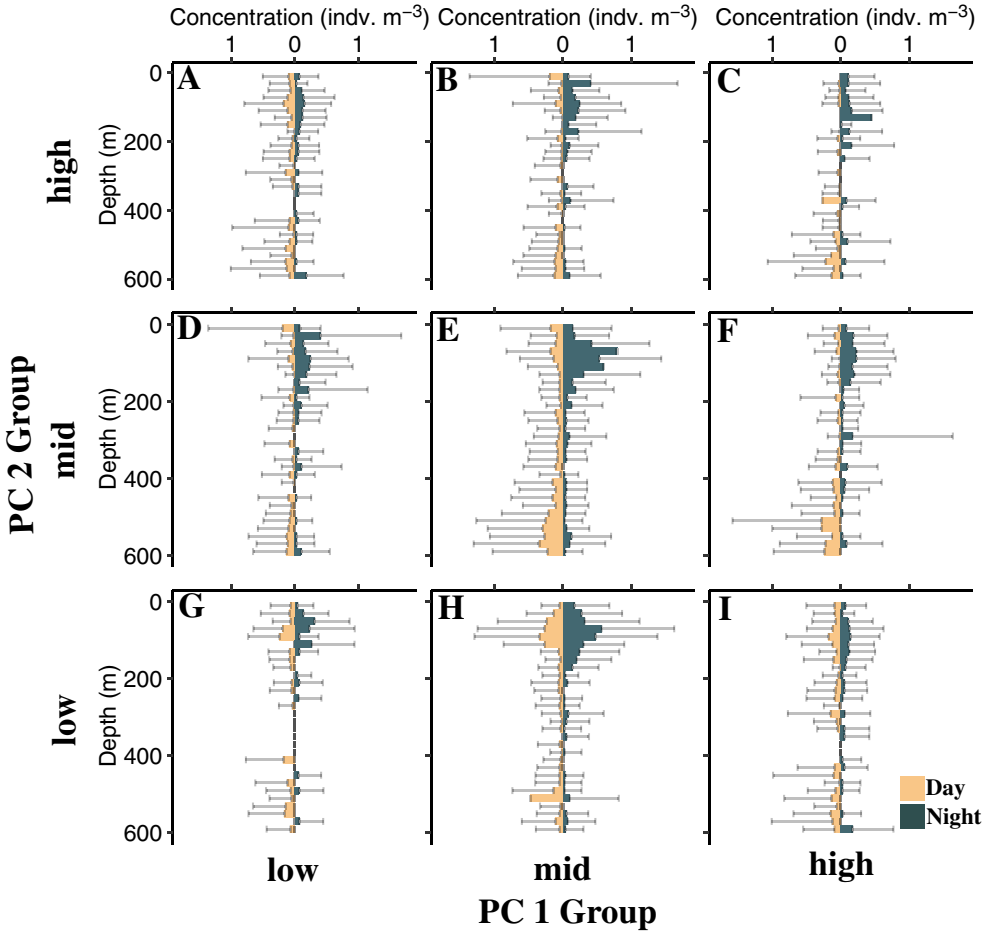

Fig. 3. Average vertical profile of different copepod morphological groups. Bars display average concentration in a 20-m depth bin. On each panel, left-side bars (tan) correspond to daytime while right-side (teal) bars correspond to nighttime. Standard deviation is shown for each 20-m depth bin. Each panel corresponds to a morphological group along PC1 (size axis) and PC2 (transparency axis). (**A**) Low PC1, high PC2; (**B**) mid PC1, high PC2; (**C**) high PC1, high PC2; (**D**) low PC1, mid PC2; (**E**) mid PC1, mid PC2; (**F**) high PC1, mid PC2; (**G**) low PC1, low PC2; (**H**) mid PC1, low PC2; (**I**) high PC1, low PC2.

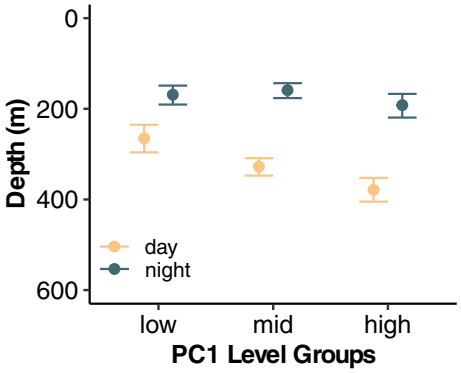

Fig. 4. Mean bootstrapped WMD and 95% CIs for copepods of different morphological groups. Low, mid, and high groups correspond to the different percentiles along PC1 from the morphospace. PC1 largely is explained by size metrics, with higher scores indicating a larger copepod.

differences were observed above 600 m (Fig. 3). For most morphological groups, there was a peak in nighttime concentration in the lower epipelagic (50–200 m). Similarly, there was a decrease in average daytime concentration over the same region. This pattern is particularly apparent for the groups which are mid and high on both PCs (Fig. 3B,C,E,F). Across all groups, both average daytime and nighttime concentration were low in the upper mesopelagic (200–300 m). Then, there was a peak in average daytime concentration in the depth bins in the mid-mesopelagic (400–600 m).

WMD analysis

The bin-constrained bootstrap approach provided a direct method to compare DVM between groups. Size (PC1) had a clear effect on DVM magnitude. First, for all PC1 groups, daytime WMD bootstrapped 95% CIs were deeper and non-overlapping with the nighttime 95% CIs (Fig. 4). This indicates a clear DVM pattern. However, the differences in day and night CIs varied between morphological groups. All PC1 groups had a similar, overlapping nighttime 95% CI in the lower epipelagic (~ 145–200 m). However, there was a clear difference in the depth of the daytime 95% CIs. The small (low PC1) group had the shallowest 95% CI (235.2–296.0 m). The mid PC1 group's daytime 95% CI was slightly deeper (309.0–347.3 m). The large (high PC1) group daytime 95% CI was even lower (352.3–405.0 m).

When considering the influence of transparency (PC2) on DVM magnitude, we compared PC2 groups within their PC1 grouping. This approach was warranted because of the tendency for size to have a slight effect on transparency (Fig. 2). At this level of comparison, there were several notable trends. For the smaller copepods (low PC1), once the data were split into PC2 groups, the wider 95% CIs indicate little to no DVM signal. Generally, the daytime 95% CIs and nighttime 95% CIs are overlapping or near-overlapping (Fig. 5A). With mid-sized copepods, there was a clear DVM signal. However, all PC2 groups appeared to have a similar DVM magnitude with each group's daytime 95% CIs overlapping with each other (Fig. 5B). There was a difference in DVM magnitude across PC2 groups within the largest copepods. The more transparent copepods (low PC2 group) showed no DVM signal, with a shallow daytime WMD. However, the darker copepods (mid and high PC2 groups) had deeper daytime WMDs (Fig. 5C).

Discussion

Copepod morphospace and quantifying DVM

In this study, we built on methods for describing morphospaces from similar in situ imaging studies (Trudnowska et al. 2021; Vilgrain et al. 2021; Sonnet et al. 2022). The PCA-defined morphospace with the present data aligns well with the prior applications. Interestingly, the proportion of morphological variation explained by each axis in the morphospace defined on Arctic copepods by Vilgrain et al. (2021) is extremely similar to the morphospace axes in this study. This similarity is striking considering the vastly different copepod community compositions between the Arctic Ocean and subtropical gyres (Soviadan et al. 2022). The similarity of morphospaces could also be an artifact of the

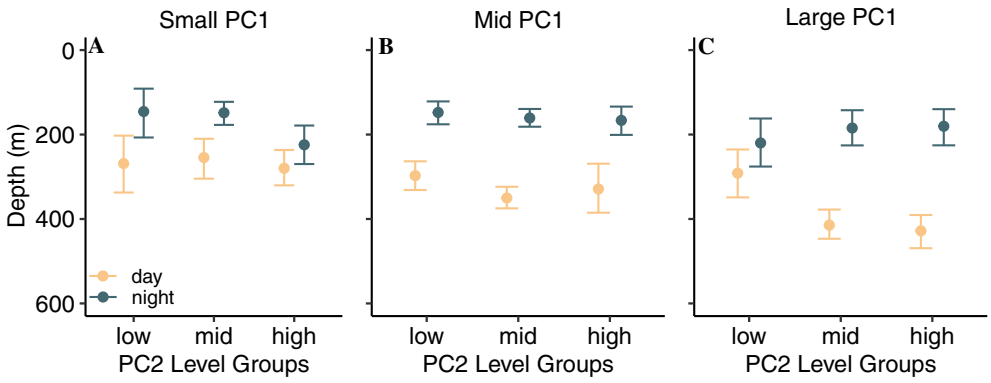

Fig. 5. Mean bootstrapped WMD and 95% CIs shown by copepod morphological groups along PC2 (transparency). Each panel represents a different size group of copepods (PC1 groups).

similarity of input data. Given the UVP has a limited range of observable size classes (Picheral et al. 2010), only copepods above a certain size were fed into both PCAs. Alternatively, the similarity of studies suggest that copepod morphological variation might be well described by these two primary axes. Sonnet et al. (2022) used phytoplankton images to investigate how a morphospace could be used to evaluate community composition changes over time. Comparisons of copepod morphospaces across temporal and spatial scales may offer a useful metric for answering biogeographic and ecological questions.

Although the UVP provides some methodological challenges to quantifying DVM, the pattern of DVM described in this study is consistent with the commonly observed nocturnal DVM pattern (Bianchi and Mislan. 2016; Bandara et al. 2021). The average vertical profiles display a clear day/night difference (Fig. 3). However, in each 20-m depth bin there was large variation, often exceeding the average concentration. This large variation was expected. There can be considerable variation between UVP estimates of zooplankton abundance (Barth and Stone 2022). In addition, in this study we pooled casts across multiple seasons. Variability in copepod DVM has been described across seasons (Whitmore and Ohman 2021). However, in the Sargasso Sea, while there is seasonal variation in DVM biomass (Behrenfeld 2014), there is no record of variation in DVM magnitude. Other studies describing DVM in the region have also pooled across seasons using net data (Ivory et al. 2019). Thus, while pooling across seasons may have introduced some variability in our WMD estimates, the DVM signal was still well described by the UVP. Previous studies using in situ imaging have also noted a signal of DVM with copepods (Pan et al. 2018; Whitmore and Ohman 2021). Yet due to small and uneven sampling, it can be a challenge to quantify DVM using in situ imaging. As presented in this study, bin-constrained bootstrapping offers a robust method to quantify WMD and investigate DVM hypotheses.

Morphological variation in DVM

The results presented in this study provide new perspective on how traits influence DVM patterns. Consistent with the size-based hypothesis (H1), we documented a clear effect in which larger copepods migrated further. This finding is consistent with several studies which have documented a size-dependent relationship for copepod DVM (Ohman and Romagnan 2016; Aarflot et al. 2019; Pinti et al. 2019). Ohman and Romagnan (2016) noted that moderate-size copepods had the largest migrations. Although this may seem contradictory to the present study, the difference between study systems needs be taken into account. The copepods described in the large (high PC1) group had a mean Feret diameter of nearly 5 mm. Conversely, in Ohman and Romagnan's (2016) study the "moderate" copepods ranged from 4 to 6 mm.

The transparency-based hypothesis (H2) was only supported by patterns within the large copepod group. The large but more transparent copepods (low PC2, high PC1) did not have a detectable DVM signal. Yet the darker copepods (mid and high PC2) had a large DVM signal. It should be noted that the gray-value recorded by the UVP may be indicative of many features which influence copepod pigmentation, including pigmentation, egg-sacs, and gut contents (Vilgrain et al. 2021). Thus, while our observation is consistent with both the predator-avoidance and the hunger-satiation hypotheses, we cannot distinguish exactly why the large, more transparent copepods do not migrate. One possibility is that these copepods have empty gut contents, and thus are less transparent and motivated to feed near the surface. However, it is also plausible that the difference in transparency is driven by taxonomic differences in pigmentation. UVP images of copepods are generally unidentifiable to higher taxonomic resolution. However, it is likely that the majority of copepod images were Calanoida, which are consistently reported as the dominant copepod group in the Sargasso Sea (Deevey and Brooks 1977; Ivory et al. 2019; Blanco-Bercial 2020). In addition, a long-term analysis of net-collected data reported only Calanoida to show a significant DVM signal (Ivory et al. 2019). However, within this group, there is extreme diversity (Deevey and Brooks 1977; Blanco-Bercial 2020). In a metabarcoding study of the epipelagic mesozooplankton community, Blanco-Bercial (2020) reported *Pleuromamma* spp., Euchaetidae, and Eucalanoidea to show higher nighttime relative abundance. Alternatively, Calanidae were described to occupy the surface waters at daytime. Thus, while the present study cannot make direct conclusions as to taxonomic variation, it is likely a driving factor in DVM variability across the observed morphological groups.

Hays (2003) described that copepod pigmentation could explain increased DVM with small (< 1 mm) copepods. Thus, it was surprising that there was no effect of transparency on DVM magnitude in the smaller morphology group. One possibility is that the small, transparent copepods were not well sampled by the UVP (Fig. 2). Due to the conservative nature of the bootstrapping WMD approach utilized in this study, sampling deficits would broaden the 95% WMD CIs, reducing the ability to resolve trends. However, there is no observable trend to suggest the lack of DVM signal is simply a methodological artifact. Alternatively, there are several possible explanations for why there is no effect of transparency for the smaller copepod morphological groups. First, it should be noted that while both the small-sized (low PC1) and mid-sized (mid-PC1) group showed no variation in DVM patterns across PC2, the mid-sized group consistently showed a strong DVM signal while the small-sized group did not. Among the small-sized group, there was little observable DVM across all transparency groupings. It may be that these copepods have a low visual-predator risk regardless of their transparency level. Ohman and Romagnan's (2016) study in the California Current observed that the smallest copepods (< 1.5 mm) displayed no DVM signal. Although these copepods

may have reduced predator risk, it may also be that they simply are weaker swimmers and cannot reasonably migrate as large of distances as bigger copepods can.

The mid-sized copepods display a clear DVM signal across all transparency groupings. This suggests that mid-sized copepods do not relieve their predation risk through increased transparency. This is counterintuitive to the observation that the large, transparent copepods have a reduced DVM signal. In addition, the transparent, mid-sized copepods migrating while the transparent, large ones do not, directly contradicts the predator-avoidance hypothesis. It is worth noting that DVM behavior can also vary greatly across species. Within migrating nekton, there has been mixed support described for the hunger-satiation hypothesis, depending on taxa (Bos et al. 2021). Thus, again it may be taxonomic variation which can explain deviations in expected DVM patterns. In addition, other mechanisms influencing DVM, asides from top-down factors may be at play. Williamson et al. (2011) provide support for the transparency-regulator hypothesis of DVM, which suggests both top-down factors and environmental factors such as UV-radiation influence DVM behavior. In the Sargasso Sea, there is extreme water clarity which would suggest UV-radiation may play a role in DVM behavior. However, none of our findings suggest that more pigmented copepods migrate less than transparent ones, regardless of size. Yet, across all copepod morphological groups, abundances were highest in the mid-to-lower mesopelagic and low in the surface layers (Fig. 2). Thus, the copepods imaged in this study are likely already at layers below where UV damage is a major factor. Furthermore, the deep Chl *a* maximum regularly extended into low epipelagic (Supplementary Fig. S2), providing sufficient food where UV irradiance is low. Nonetheless, while UV may not be a primary factor, the notion that there are multiple factors influencing DVM should be considered.

Conclusion

Overall, our results reveal a complex dynamic between copepod traits and DVM behavior. This study provided new insight into the DVM dynamics in oligotrophic gyres. Although many studies have established size as a major trait influencing DVM, investigations into other traits are more limited. Here, we support the prevailing notion that size has large consequences for DVM behavior. We also show that transparency has an effect on DVM for some size groups. However, determining exactly which drivers determine why copepods with different traits undergo DVM remains elusive. Although these findings are largely consistent with the predator-avoidance hypothesis and prevailing DVM theory, they highlight the need for more detailed analyses. As plankton in situ imaging tools are used more commonly by oceanographers, larger datasets will facilitate new investigations. Additionally, improved resolution of sampling tools may better determine taxonomic variation. Collaborations between oceanographers, plankton ecologists, and visual ecologists may better resolve how traits influence trade-offs in DVM behavior. Understanding these dynamics will be critical to predicting changes with a changing ocean.

Data availability statement

All data used in this project are hosted on Ecopart (https://ecopart.obs-vlfr.fr/). Data in its raw form can be accessed from their portal. However, all summary and intermediate data products, as well as code, are publicly available on GitHub (https://github.com/TheAlexBarth/DVM_Migration-Morphology). Intermediate data products are formatted as R Data Structure objects, other formats are available on request.

References

Aarflot, J. M., D. L. Aksnes, A. F. Opdal, H. R. Skjoldal, and Ø. Fiksen. 2019. Caught in broad daylight: Topographic constraints of zooplankton depth distributions. Limnol. Oceanogr. **64**: 849–859. doi:10.1002/lno.11079

Aksnes, D. L., and A. C. W. Utne. 1997. A revised model of visual range in fish. Sarsia **82**: 137–147. doi:10.1080/00364827.1997.10413647

Archibald, K. M., D. A. Siegel, and S. C. Doney. 2019. Modeling the impact of zooplankton diel vertical migration on the carbon export flux of the biological pump. Global Biogeochem. Cycl. **33**: 181–199. doi:10.1029/2018GB005983

Atkinson, A., P. Ward, R. Williams, and S. A. Poulet. 1992. Diel vertical migration and feeding of copepods at an oceanic site near South Georgia. Mar. Biol. **113**: 583–593. doi:10.1007/BF00349702

Bandara, K., Ø. Varpe, R. Ji, and K. Eiane. 2019. Artificial evolution of behavioral and life history strategies of high-latitude copepods in response to bottom-up and top-down selection pressures. Prog. Oceanogr. **173**: 134–164. doi:10.1016/j.pocean.2019.02.006

Bandara, K., Ø. Varpe, L. Wijewardene, V. Tverberg, and K. Eiane. 2021. Two hundred years of zooplankton vertical migration research. Biol. Rev. **96**: 1547–1589. doi:10.1111/brv.12715

Barth, A., and J. Stone. 2022. Comparison of an in situ imaging device and net-based method to study mesozooplankton communities in an oligotrophic system. Front. Mar. Sci. **9**: 898057. doi:10.3389/fmars.2022.898057

Behrenfeld, M. J. 2014. Climate-mediated dance of the plankton. Nat. Clim. Change **4**: 880–887. doi:10.1038/nclimate2349

Behrenfeld, M. J., and others. 2019. Global satellite-observed daily vertical migrations of ocean animals. Nature **576**: 257–261. doi:10.1038/s41586-019-1796-9

Bianchi, D., and K. A. S. Mislan. 2016. Global patterns of diel vertical migration times and velocities from acoustic data. Limnol. Oceanogr. **61**: 353–364. doi:10.1002/lno.10219

Blanco-Bercial, L. 2020. Metabarcoding analyses and seasonality of the zooplankton community at BATS. Front. Mar. Sci. **7**: 173. doi:10.3389/fmars.2020.00173

Bos, R. P., T. T. Sutton, and T. M. Frank. 2021. State of satiation partially regulates the dynamics of vertical migration. Front. Mar. Sci. **8**: 607228. doi:10.3389/fmars.2021.607228

Brierley, A. S. 2014. Diel vertical migration. Curr. Biol. **24**: R1074–R1076. doi:10.1016/j.cub.2014.08.054

Cohen, J. H., and R. B. Forward Jr. 2009. Zooplankton diel vertical migration: A review of proximate control. Oceanogr. Mar. Biol. **47**: 77–109.

Deevey, G. B., and A. L. Brooks. 1977. Copepods of the sargasso sea off Bermuda: Species composition, and vertical and seasonal distribution between the surface and 2000 m. Bull. Mar. Sci. **27**: 256–291.

Enright, J. T. 1977. Diurnal vertical migration: Adaptive significance and timing. Part 1. Selective advantage: A metabolic model1. Limnol. Oceanogr. **22**: 856–872. doi:10.4319/lo.1977.22.5.0856

Ewald, W. F. 1912. On artificial modification of light reactions and the influence of electrolytes on phototaxis. J. Exp. Zool. **13**: 591–612. doi:10.1002/jez.1400130405

Gorsky, G., and others. 2010. Digital zooplankton image analysis using the ZooScan integrated system. J. Plankton Res. **32**: 285–303. doi:10.1093/plankt/fbp124

Hays, G. C. 2003. A review of the adaptive significance and ecosystem consequences of zooplankton diel vertical migrations. Springer, p. 163–170.

Hays, G. C., C. A. Proctor, A. W. G. John, and A. J. Warner. 1994. Interspecific differences in the diel vertical migration of marine copepods: The implications of size, color, and morphology. Limnol. Oceanogr. **39**: 1621–1629. doi:10.4319/lo.1994.39.7.1621

Ivory, J. A., D. K. Steinberg, and R. J. Latour. 2019. Diel, seasonal, and interannual patterns in mesozooplankton abundance in the sargasso sea. ICES J. Mar. Sci. **76**: 217–231. doi:10.1093/icesjms/fsy117

Kelly, T. B., P. C. Davison, R. Goericke, M. R. Landry, M. D. Ohman, and M. R. Stukel. 2019. The importance of mesozooplankton diel vertical migration for sustaining a mesopelagic food web. Front. Mar. Sci. **6**: 508. doi:10.3389/fmars.2019.00508

Kessler, K., R. S. Lockwood, C. E. Williamson, and J. E. Saros. 2008. Vertical distribution of zooplankton in subalpine and alpine lakes: Ultraviolet radiation, fish predation, and the transparency-gradient hypothesis. Limnol. Oceanogr. **53**: 2374–2382. doi:10.4319/lo.2008.53.6.2374

Lampert, W. 1989. The adaptive significance of diel vertical migration of zooplankton. Funct. Ecol. **3**: 21–27. doi:10.2307/2389671

Liu, Y., J. Guo, Y. Xue, C. Sangmanee, H. Wang, C. Zhao, S. Khokiattiwong, and W. Yu. 2022. Seasonal variation in diel vertical migration of zooplankton and micronekton in the Andaman sea observed by a moored ADCP. Deep Sea Res. I Oceanogr. Res. Pap. **179**: 103663. doi:10.1016/j.dsr.2021.103663

Maas, A. E., L. Blanco-Bercial, A. Lo, A. M. Tarrant, and E. Timmins-Schiffman. 2018. Variations in copepod proteome and respiration rate in association with diel vertical migration and circadian cycle. Biol. Bull. **235**: 30–42. doi:10.1086/699219

McLaren, I. A. 1963. Effects of temperature on growth of zooplankton, and the adaptive value of vertical migration. J. Fish. Res. Board Can. **20**: 685–727. doi:10.1139/f63-046

McLaren, I. A. 1974. Demographic strategy of vertical migration by a marine copepod. Am. Nat. **108**: 91–102.

Ohman, M. D. 1990. The demographic benefits of diel vertical migration by zooplankton. Ecol. Monogr. **60**: 257–281. doi:10.2307/1943058

Ohman, M. D. 2019. A sea of tentacles: Optically discernible traits resolved from planktonic organisms in situ H. Browman [ed.]. ICES J. Mar. Sci. **76**: 1959–1972. doi:10.1093/icesjms/fsz184

Ohman, M. D., and J.-B. Romagnan. 2016. Nonlinear effects of body size and optical attenuation on diel vertical migration by zooplankton. Limnol. Oceanogr. **61**: 765–770. doi:10.1002/lno.10251

Ohman, M. D., J. A. Runge, E. G. Durbin, D. B. Field, and B. Niehoff. 2002. On birth and death in the sea. Hydrobiologia **480**: 55–68. doi:10.1023/A:1021228900786

Pan, J., F. Cheng, and F. Yu. 2018. The diel vertical migration of zooplankton in the hypoxia area observed by video plankton recorder. Indian J. Mar. Sci. **47**: 1353–1363.

Pearre, S. 2003. Eat and run? The hunger/satiation hypothesis in vertical migration: History, evidence and consequences. Biol. Rev. **78**: 1–79. doi:10.1017/S146479310200595X

Picheral, M., S. Colin, and J.-O. Irisson. 2017. EcoTaxa, a tool for the taxonomic classification of images. [Accessed 2023 June 11]. https://ecotaxa.obs-vlfr.fr/

Picheral, M., L. Guidi, L. Stemmann, D. M. Karl, G. Iddaoud, and G. Gorsky. 2010. The underwater vision profiler 5: An advanced instrument for high spatial resolution studies of particle size spectra and zooplankton. Limnol. Oceanogr. Methods **8**: 462–473. doi:10.4319/lom.2010.8.462

Pinti, J., T. Kiørboe, U. H. Thygesen, and A. W. Visser. 2019. Trophic interactions drive the emergence of diel vertical migration patterns: A game-theoretic model of copepod communities. Proc. R. Soc. B Biol. Sci. **286**: 20191645. doi:10.1098/rspb.2019.1645

Ringelberg, J. 2009. Diel vertical migration of zooplankton in lakes and oceans: Causal explanations and adaptive significances. Springer Science & Business Media.

Robison, B. H., R. E. Sherlock, K. R. Reisenbichler, and P. R. McGill. 2020. Running the gauntlet: Assessing the threats to vertical migrators. Front. Mar. Sci. **7**: 64. doi:10.3389/fmars.2020.00064

Schnetzer, A., and D. K. Steinberg. 2002. Active transport of particulate organic carbon and nitrogen by vertically migrating zooplankton in the Sargasso Sea. Mar. Ecol. Prog. Ser. **234**: 71–84. doi:10.3354/meps234071

Siegel, D. A., T. DeVries, I. Cetinić, and K. M. Bisson. 2023. Quantifying the ocean's biological pump and its carbon cycle impacts on global scales. Annu. Rev. Mar. Sci. **15**: 329–356. doi:10.1146/annurev-marine-040722-115226

Sonnet, V., L. Guidi, C. B. Mouw, G. Puggioni, and S.-D. Ayata. 2022. Length, width, shape regularity, and chain structure: Time series analysis of phytoplankton morphology from imagery. Limnol. Oceanogr. **67**: 1850–1864. doi:10.1002/lno.12171

Soviadan, Y. D., and others. 2022. Patterns of mesozooplankton community composition and vertical fluxes in the global ocean. Prog. Oceanogr. **200**: 102717. doi:10.1016/j.pocean.2021.102717

Steinberg, D. K., C. A. Carlson, N. R. Bates, S. A. Goldthwait, L. P. Madin, and A. F. Michaels. 2000. Zooplankton vertical migration and the active transport of dissolved organic and inorganic carbon in the Sargasso Sea. Deep Sea Res. I Oceanogr. Res. Pap. **47**: 137–158. doi:10.1016/S0967-0637(99)00052-7

Steinberg, D. K., C. A. Carlson, N. R. Bates, R. J. Johnson, A. F. Michaels, and A. H. Knap. 2001. Overview of the US JGOFS Bermuda Atlantic Time-series Study (BATS): A decade-scale look at ocean biology and biogeochemistry. Deep Sea Res. II Topic. Stud. Oceanogr. **48**: 1405–1447. doi:10.1016/S0967-0645(00)00148-X

Steinberg, D. K., and M. R. Landry. 2017. Zooplankton and the ocean carbon cycle. Annu. Rev. Mar. Sci. **9**: 413–444. doi:10.1146/annurev-marine-010814-015924

Szeligowska, M., E. Trudnowska, R. Boehnke, A. M. Dąbrowska, K. Dragańska-Deja, K. Deja, M. Darecki, and K. Błachowiak-Samołyk. 2021. The interplay between plankton and particles in the Isfjorden waters influenced by marine- and land-terminating glaciers. Sci. Total Environ. **780**: 146491. doi:10.1016/j.scitotenv.2021.146491

Trudnowska, E., L. Lacour, M. Ardyna, A. Rogge, J. O. Irisson, A. M. Waite, M. Babin, and L. Stemmann. 2021. Marine snow morphology illuminates the evolution of phytoplankton blooms and determines their subsequent vertical export. Nat. Commun. **12**: 2816. doi:10.1038/s41467-021-22,994-4

Turner, J. 2004. The importance of small planktonic copepods and their roles in pelagic marine food webs. Zool Stud. **43**: 255–266.

Vilgrain, L., F. Maps, M. Picheral, M. Babin, C. Aubry, J.-O. Irisson, and S.-D. Ayata. 2021. Trait-based approach using in situ copepod images reveals contrasting ecological patterns across an Arctic ice melt zone. Limnol. Oceanogr. **66**: 1155–1167. doi:10.1002/lno.11672

Whitmore, B. M., and M. D. Ohman. 2021. Zooglider-measured association of zooplankton with the fine-scale vertical prey field. Limnol. Oceanogr. **66**: 3811–3827. doi:10.1002/lno.11920

Williamson, C. E., J. M. Fischer, S. M. Bollens, E. P. Overholt, and J. K. Breckenridge. 2011. Toward a more comprehensive theory of zooplankton diel vertical migration: Integrating ultraviolet radiation and water transparency into the biotic paradigm. Limnol. Oceanogr. **56**: 1603–1623. doi:10.4319/lo.2011.56.5.1603

Zaret, T. M., and J. S. Suffern. 1976. Vertical migration in zooplankton as a predator avoidance mechanism1. Limnol. Oceanogr. **21**: 804–813. doi:10.4319/lo.1976.21.6.0804

Acknowledgments

Field work for this project was supported by the Bermuda Atlantic Time Series Study through NSF OCE 1756105 and NSF OCE 1756312. We would also like to thank the BATS research technicians, marine technicians, and crew of the R/V Atlantic Explorer. Dr. Ryan Rykaczewski assisted with the initial set-up of the UVP. Dr. Leo Blanco-Bercial and Dr. Amy Maas both valuable insight and guidance on the analysis.

Conflict of Interest

None declared.

Submitted 15 May 2023
Revised 09 September 2023
Accepted 04 November 2023

Associate editor: Thomas Kiørboe